Solar Energy Materials & Solar Cells 299 (2026) 114228

Contents lists available at ScienceDirect

Solar Energy Materials and Solar Cells

journal homepage: www.elsevier.com/locate/solmat

Low-filled electrically conductive adhesives based on silver-coated glass and copper particles

Marianne Kronsbein [a,*], Leonhard Böck [b], Torsten Rößler [b], Norbert Willenbacher [a]

[a] Karlsruhe Institute of Technology, Gotthard-Franz-Straße 3, 76131, Karlsruhe, Germany
[b] Fraunhofer Institute for Solar Energy Systems, Heidenhofstraße 2, 79110, Freiburg, Germany

A B S T R A C T

Replacing silver in solar module production is the hot topic in metallization and interconnection development. Whereas in metallization mainly silver-coated copper is utilized, the lower electrical requirements for cell interconnection, open up the opportunity to utilize particles with non-conductive cores as well. This study focuses on the development and characterization of an electrically conductive adhesive (ECA) for the shingled cell interconnection based on silver-coated glass and silver-coated copper particles, respectively. The formulated low-filled ECAs were stabilized against sedimentation using a halogen-based additive.

The silver-coated glass particles show good compatibility with the utilized epoxy resin. Employing a mixture of silver-coated glass particles and silver flakes, the silver content in the ECA can be reduced to 25 wt% and the mechanical properties can be adjusted by the fraction of glass particles used. In shingled modules such an ECA shows the same stable performance as the reference based on pure silver particles.

An ECA with only 7 wt% silver was formulated using silver-coated copper particles meeting all requirements for solar cell shingling. Shingled modules build from such an ECA show promising initial efficiency. Damp heat 500 was passed comparable to the silver reference, indicating oxidation stability. However, degradation during accelerated thermal cycling 200 is believed to originate from remaining issues with curing.

This study shows, that by carefully adjusting polymer, particles and additives the silver consumption in ECAs can be significantly reduced without any losses in interconnection performance.

1. Introduction

The International Technology Roadmap for Photovoltaic (ITRPV) identifies silver as the “most process-critical and most expensive non-silicon material” [1] at cell level. In 2024, the photovoltaic (PV) industry accounted for approximately 19% of global silver demand. Although the average silver consumption per cell is declining—helping to offset rising PV deployment—ongoing large-scale investments in PV infrastructure, primarily driven by climate targets, may continue to place significant strain on the silver supply chain [2]. Consequently, further reductions in silver consumption, particularly in cell metallization pastes, are essential.

Electrically conductive adhesives (ECAs) have emerged as promising alternatives to solder in cell interconnection technologies. These adhesives are thermosetting polymer-based composites filled with conductive particles and are increasingly employed to attach ribbons to busbars on solar cells [3], for contacting back-contact solar cells to conductive backsheets [4], or to directly interconnect the cells in shingled module architectures [5]. Conventional ECAs typically contain silver particles at concentrations above the percolation threshold for electrical conductivity, which depends on filler morphology and generally falls between 15 and 30 vol% (equivalent to 60–80 wt%) [6]. Therefore, ECAs present an additional source of silver in PV.

To address the high cost and limited availability of silver, research and commercial efforts have explored replacing silver with alternative conductive fillers. Tables 1 and 2 summarize commercially available and literature-reported ECAs with volume resistivity below 10^{-2} Ω cm. Among the explored alternatives, copper — most commonly used as silver-coated copper particles — has emerged as the predominant substitute due to its favourable electrical properties and significantly lower cost. The ITRPV also anticipates a growing role for copper in future metallization pastes. At present, copper remains an abundant and economically viable alternative to silver [7]. However, long-term availability may become a concern: Nobel laureate and former U.S. Secretary of Energy Steven Chu has projected potential copper shortages by the end of the century, driven by increasing global demand for electrification [8]. Other materials, including nickel, aluminium, and carbon have also been investigated as conductive core particles for use in ECAs.

Some approaches further minimize the use of conductive metals by

* Corresponding author.
E-mail address: marianne.kronsbein@kit.edu (M. Kronsbein).

https://doi.org/10.1016/j.solmat.2026.114228
Received 12 December 2025; Received in revised form 5 February 2026; Accepted 6 February 2026
Available online 10 February 2026

utilizing non-conductive core particles, such as glass spheres, coated with a thin silver layer. For instance, an ECA based on silver-coated glass microspheres with a volume resistivity of 1.5×10^{-3} Ω cm has been developed [10]. Nevertheless, nearly all ECAs rely on high filler loadings to achieve sufficient conductivity. While increased filler content enhances electrical pathways, it often compromises the adhesive's mechanical properties. Moreover, the sustainable approach is to utilize as little valuable materials, both silver and copper, as possible.

This study aims to develop low-filled ECAs with significantly reduced silver and total filler content, while still meeting the stringent electrical and mechanical requirements for shingled solar cell interconnection. These include a yield stress between 10 and 100 Pa in the uncured state, rapid curing within seconds at low temperatures, volume resistivity below 10^{-2} Ω cm, and lap-shear strength exceeding 10 MPa [26]. This study is based on a well characterized low-filled silver-epoxy system [26]. Here, we outline how substantial further silver reduction is achieved by utilizing silver-coated glass and silver-coated copper particles instead of pure silver particles. Halogen-additives stabilize the formulations preventing sedimentation in low-filled, uncured state ECAs and provide low resistivity and high mechanical strength in the cured state. Furthermore, we demonstrate the general suitability of such ECAs for shingled solar cell interconnection.

2. Material and methods

2.1. Material

A two-component thermosetting epoxy resin and silver flakes (Ag flakes) were supplied by PROTAVIC INTERNATIONAL (France). Silver-coated copper particles (AgCu0608-15, 15 wt% Ag, specific surface area (SSA) = 0.63 m^2/g) were provided by AMES Advanced Materials Cop. (US) and are denoted here as Ag@Cu. Silver coated-glass particles (SG05TF40, 40 wt% Ag) were purchased from PI-KEM Hart (UK) and are denoted here as Ag@glass. All particles were used as received.

2.2. Particle characterization

Scanning Electron Microscopy (SEM) was performed using a Phenom Pharos G2 (Thermo Fisher Scientific, Germany). Particle size distribution was determined by laser diffraction using a HELOS system equipped with a RODOS dry disperser (SympaTEC, Germany). Thermogravimetric analysis (TGA) was conducted using a TGA 5500 (TA Instruments) under air and nitrogen atmosphere. Differential Scanning Calorimetry (DSC) measurements were carried out using a DSC 214 Polyma (Netzsch, Germany) in closed sample pans. TGA and DSC measurements were performed from room temperature to 400 °C at a heating rate of 10 K/min. For DSC analysis, baseline correction was performed by fitting a 3rd-degree polynomial to the curve while excluding the temperature range of the peaks (100-250 °C); the fitted baseline was subsequently subtracted from the original curve.

2.3. ECA preparation

Epoxy resin and particles were mixed for 2 min at 2000 rpm using a SpeedMixer DAC 150.1 FVZ (Hauschild, Germany). Additives were then added and mixed for an additional time of 1 min. In the final step, the catalyst was added and mixed for 1 min. For resistivity measurements, three ECA lines with a thickness of 100 μm and a width of 4 mm were stencil-printed onto glass slides and cured for 2 min at 150 °C on a heat plate. Samples for mechanical testing were cured for 10 min at 150 °C in an oven. A detailed study on the influence of curing time and temperature for silver-filled ECAs based on the epoxy resin and Ag flakes also used here is reported elsewhere [26].

2.4. ECA characterization

Rheological measurements were performed using a MARS rotational rheometer (Thermo Fisher Scientific, Germany) equipped with a plate-plate geometry (20 mm diameter) and gap height of 1 mm. For yield stress determination, shear stress was increased stepwise from 0.1 to 1000 Pa in 81 logarithmic steps. The yield stress was defined as the intersection point of the linear fits to the elastic and to the viscous region in a double logarithmic deformation-stress-diagram [27]. Viscosity was determined by increasing the shear rate from 0.1 to 1000 1/s in 41 logarithmic steps. Each rheological measurement was carried out three times per sample.

Volume resistivity was measured using a 4-point probe setup with a 2450 SourceMeter (Keithley, US) and a probe spacing of 15 mm. Nine data points were taken per sample. Contact resistivity was measured according to Ref. [28]. Lap-shear strength was determined based on ASTM D1002 [29]. Carbon steel was used as substrate for lap-shear test samples. The bonding area was approximately 15 mm^2. Three specimens per ECA were measured using a universal tensile testing machine TA.XT plus Texture Analyser (Stable Micro Systems, UK) at a crosshead speed of 0.2 mm/s. For Young's Modulus determination, 15 samples were prepared in accordance with DIN EN ISO 20753, type A22 [30], and pulled at a crosshead speed of 0.01 mm/s. Mean values and standard deviation were calculated for all parameters.

2.5. Module preparation and testing

For module testing, mass-produced Passivated Emitter and Rear Cell

Table 1
Commercially available ECAs with conductive particles that are not made of pure silver; note: X@Y refers to X coated on Y, for X-Y type fillers structure is not specified by the manufacturer.

Manufacturer	Product	Polymer	Fill grade	Filler	Cure schedule	Resistivity/10^{-3} Ω cm	Ref
Nagase	CA-260	Epoxy	45-70 wt% Ag	Ag@X (non Cu)	30 s @ 150 °C/5 min @ 120 °C	0.15	[9]
Nagase	CA-183	Epoxy	10-30 wt% Ag, 45-70 wt% Cu	Ag@Cu	20 min @ 100 °C/1 min @ 150 °C	0.9	[9]
atom adhesives	AA-DUCT GS1	Epoxy	50-70% Ag coated ceramic	Ag@glass spheres	15 min @ 100 °C	1.5	[10]
United Adhesives	Eposolder 6761	Epoxy		Ag-Cu	60 min @ 125 °C	1	[11]
United Adhesives	Eposolder 6763	Epoxy		Ag-Cu	60 min @ 125 °C/30 min @ 150 °C	5	[11]
Parker	CHO-BOND 360-20	Epoxy	3-7 wt% Ag, 80-90 wt% Cu	Ag@Cu	25 min @ 115 °C	5	[12]
Masterbond	EP79FL	Epoxy		Ag@Ni	overnight @ RT + 2-3 h@110 °C	5	[13]
Holland Shielding	3991 Shieldoseal	Silicone	50-70 wt% Ni	Ni@graphite	96-144 h at RT	7.0	[14]
Soliani	CSA.SPC	Silicone		Ag-Cu	72 h @ RT	8	[15]
Soliani	CSA.SNK	Silicone		Ag-Ni	72 h @ RT	8	[15]
Soliani	CSA.SPA	Silicone		Ag-Al	72 h @ RT	10	[15]

(PERC) cells in G1 5th (158.75 × 31.75 mm^2) format were used. The initial host cell efficiency (before dicing) was 21.8%. Three types of electrically conductive adhesives were evaluated for cell interconnection. The commercially available ECA PROTAVIC® ACE 10720 (PROTAVIC INTERNATIONAL, France) filled with 5-10 vol% Ag flakes was used as the reference material. The Ag@glass ECA contained 3.5 vol% silver at a total filler content of 8 vol%, and the Ag@Cu ECA contained 10 vol% of Ag@Cu particles (1.7 vol% silver).

Cell interconnection was performed using a prototype shingle stringer from M10 Industries. The ECA was dispensed on the cells as continuous lines, covering the entire busbar. ECA curing was performed using an infrared lamp setup with a maximum process temperature of 140 °C. The maximum temperature was monitored by temperature-measuring strips attached to the rear side of dummy cells. Each string consisted of six shingle cells. The modules were laminated in a glass-backsheet configuration using an industrial laminator (Bürkle Ypsator M-LAPV 1222-HKV). The lamination temperature was 155 °C. Ethylene-vinyl acetate foils (F406PS for front side, F806PS for back side, Hangzhou First Applied Material) served as encapsulant material. Module *IV* characteristics were measured on a non-calibrated, xenon-lamp-based sun simulator (halm elektronik GmbH, Germany). *IV* characterization was carried out under STC (AM1.5G spectrum, 1000 W/m^2), and temperature-corrected to 25 °C using the cell temperature coefficients provided by the cell manufacturer.

Each group consisted of 12 samples, where six were intended for thermal cycling and six for temperature-humidity aging. Two additional modules containing reference ECA were set aside without aging treatment to serve as controls for estimating calendar aging effects and measurement uncertainty. To evaluate the interconnection reliability, accelerated Thermal Cycling (aTC) and Damp Heat (DH) tests were selected. The aTC test protocol employed six times faster cycling rates compared to the standard Thermal Cycling (TC) test described in IEC 61215-2 MQT 11. Comparable results between aTC and TC have been demonstrated in Ref. [31]. The DH tests followed IEC 61215-2 MQT 13. aTC aging consisted of 200 cycles and DH aging of 500 h.

3. Results and discussion

3.1. Particle characterization

In this study, three different particle types were investigated: silver flakes (Ag flakes), used as reference and additional filler; silver-coated glass flakes (Ag@glass) with a silver content of 40 wt%; and silver-coated copper flakes (Ag@Cu) with a silver content of 15 wt%. SEM images depicting the morphology of the different particles are shown in Fig. 1. All investigated particles exhibited a flake-like morphology. The Ag flakes were the thinnest and exhibited an irregular shape. The Ag@Cu particles had a similar shape but with a smoother contour. In contrast, Ag@glass particles had a more angular contour and a rather uniform thickness of app. 2 μm. Fig. 2a depicts the particle size distribution determined using laser diffraction. The reported equivalent diameters were calculated assuming spherical particles. As all investigated particles were flake-shaped, they are not characterized by a single diameter value. Nevertheless, the obtained values correlate well with the lateral particle dimensions observed in the SEM images, while the particle thickness is not adequately captured. Overall, all particles fall within a similar size range, with $x_{50,3}$ values ranging from 6.4 μm for the Ag@glass particles to 15.5 μm for the Ag flakes.

To characterize the surface chemistry of the particles, DSC and TGA measurements were performed. Fig. 2b shows the baseline-corrected heat flow for the particle samples between 75 and 300 °C, determined by DSC at a heating rate of 10 K/min. All particle types exhibited an exothermic peak in the temperature range between 150 and 250 °C. Peak temperatures were app. 180 °C for Ag@Cu and around 220 °C for Ag flakes and Ag@glass particles. In all cases, the observed peaks are relatively broad. In addition, the DSC curve of the Ag flakes exhibited a secondary exothermic peak around 270 °C.

TGA measurements (depicted in Fig. S1) confirmed the DSC results. All TGA curves revealed a mass loss in the temperature range corresponding to the exothermic peaks observed in DSC. Furthermore, the Ag@Cu particles exhibited a mass increase above approximately 230 °C, which can be attributed to the oxidation of the copper core. During particle manufacturing, fatty acids are commonly utilized as process aids to prevent cold welding during milling. Residual amounts of these organic compounds typically remain on the particle surface. The observed DSC peak temperatures and the corresponding mass losses in the TGA measurements are in good agreement with literature values reported for the thermal decomposition of such fatty acids [32,33]. Therefore, DSC and TGA results strongly indicate the presence of a thin fatty-acid-based organic layer on the surface of all investigated particle types.

Table 2
ECAs reported in literature with conductive particles that are not made of pure silver.

Polymer	Fill grade	Filler	Additive	Cure schedule	Resistivity/10^{-3} Ω cm	Ref
Epoxy	67 wt%	Cu particles	lactic acid	1 h @ 200 °C under nitrogen	0.12	[16]
Epoxy	70 wt%	Ag@Cu flakes (17.3 wt% Ag)	diisobutyl phthalate, 20 wt%	2 h @ 180 °C	0.127	[17]
Epoxy	75 wt%	Ag@Cu flakes (25 wt% Ag, 74.5 wt% Cu)	terephthalaldehyde and iodine (ratio TPTA/I_2 = 30/1)	1 h @ 150 °C	0.128	[18]
Epoxy	60 wt%	Ag@Cu powder	none	30 min @150 °C in vacuum	0.2	[19]
Epoxy	40 wt%	Submicron Ag@Cu particles (15 wt% Ag) and commercial micron Ag@Cu	palmitic acid	2 h @ 160 °C	0.468	[20]
Epoxy	70 wt%	Ag@Cu powder:	none	2 h @ 175 °C		[21]
		flake-shaped particles			1.58	
		spherical shaped-particles			3.98	
Epoxy	60 wt%	flaky and spherical Ag@Cu	none	1 h @150 °C in vacuum oven	1.95	[22]
Epoxy	70 - 85 wt	Ag-Cu particles:		30 min @ 80 °C		[23]
	%	20 wt% Ag	None		2	
		50 wt% Ag	None		1	
		30 wt% Ag	Graphite		4	
Epoxy	70 - 85 wt	flake-shaped,	None	30 min @ 80 °C	3	[24]
	%	flake- and spherical-shaped: 60:40	None		4.5	
		Ag@Cu powder (10 - 15 wt% Ag)	graphite (8 wt%)		8	
Epoxy	55 wt%	Ag@Cu flakes	None	1 h @ 200 °C	6	[25]

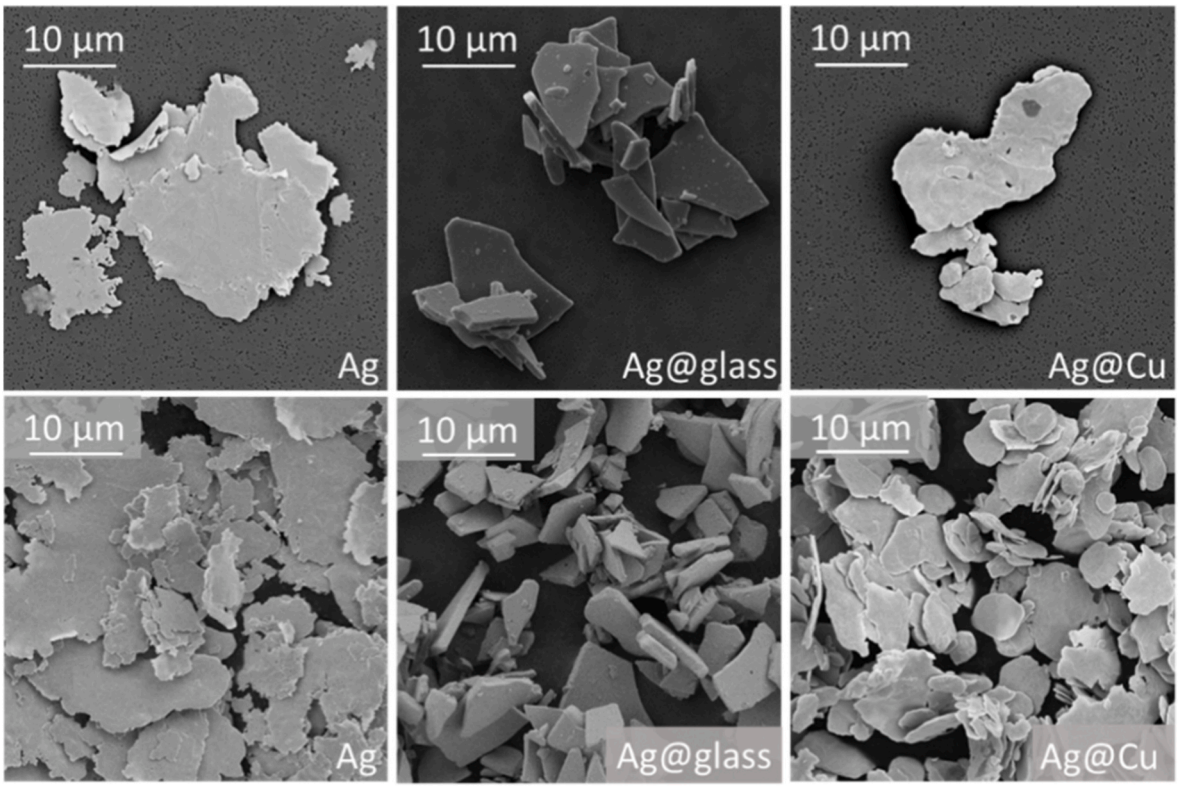

Fig. 1. SEM images of Ag, Ag@glass and Ag@Cu as single particles and particle agglomerates for comparison of morphology and particle shape of the different particle types used for ECA formulation.

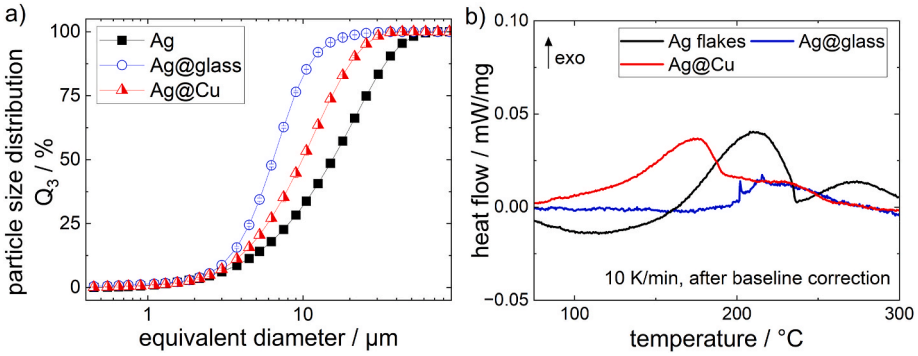

Fig. 2. a) particle size distribution Q_3 measured by laser diffraction giving the equivalent sphere diameter and b) DSC analysis in air of Ag (black), Ag@glass (blue) and Ag@Cu (red) flakes for characterization of the surface chemistry of the particles, heating rate: 10 K/min, after baseline correction, exotherm: up. (For interpretation of the references to colour in this figure legend, the reader is referred to the Web version of this article.)

3.2. ECAs based on silver-coated glass particles

In a first set of experiments, silver-coated glass particles were employed as fillers in the epoxy resin. They utilize a non-conductive core, which increases the effective volume of each particle and therefore, the number of potential contact points between the particles.

As a reference, an ECA prepared from the same epoxy resin and pure Ag flakes is reported. This formulation exhibited electrical percolation at a filler content between 10 and 15 vol%, resulting in a decrease in volume resistivity from app. 18 Ω cm at 10 vol% Ag to $(1.2 \pm 0.3)\ 10^{-2}$ Ω cm at 15 vol%, see Fig. 3a. Beyond the percolation threshold, such an ECA exhibited a yield stress, providing sedimentation stability. In contrast, Ag@glass-based ECAs without additives did not percolate within the investigated filler content range of 5 to 25 vol%. Increasing the Ag@glass content decreased the volume resistivity from 10^6 Ω cm at 5 vol% filler to 10^4 Ω cm at 25 vol%. The standard deviation increased with increasing filler content, indicating the formation of isolated conductive pathways. Simultaneously, the paste exhibited macroscopic inhomogeneities, but no measurable yield stress was observed.

Previous studies have demonstrated that halogens can significantly influence both the yield stress and the electrical conductivity of ECAs [34–36]. Yang et al. [34] reported that iodine reacts with the silver particle surface, forming silver-nano islands. Sun et al. [35] observed halogen-induced structural changes resulting in the formation of a particle network, which increased yield stress and decreased volume resistivity. More recently, Marten et al. [36] attributed similar effects to the removal of fatty acids from the particle surface and the formation of silver iodide. This modification of the surface chemistry promotes van der Waals dominated attractive particle–particle interactions and closer particle contact, thereby increasing yield stress and lowering the electrical percolation threshold. Consistent with these findings, the addition of a halogen(h)-based additive to the polymer-particle system

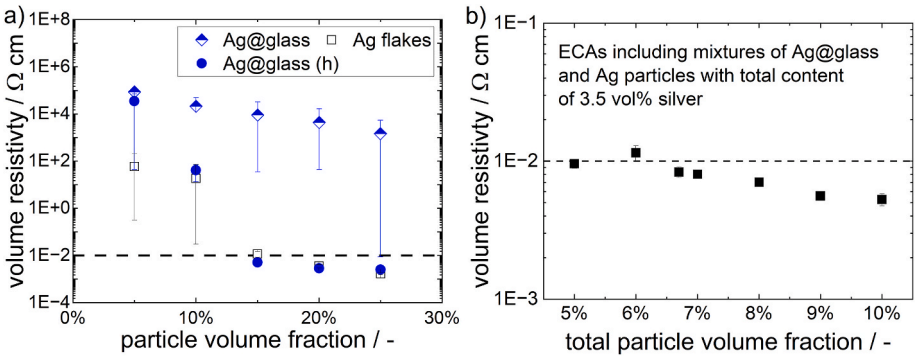

Fig. 3. Volume resisitivity of ECAs with Ag flakes (un-filled black squares) and Ag@glass (blue) without (filled circles) and with (half-filled diamonds) halogen(h)-based additives and filler content between 5 and 25 vol% b) volume resisitivity of ECAs with varying total filler content between 5 and 10 vol% comprising Ag@glass and Ag particles at different mixing ratios to contain 3.5 vol% silver, higher total particle volume fraction corresponds to a higher fraction of Ag@glass particles in the mixture; dashed lines indicate the maximum volume resistivity required for solar cell shingling. (For interpretation of the references to colour in this figure legend, the reader is referred to the Web version of this article.)

investigated here significantly altered both the percolation threshold as well as morphology of ECAs containing Ag@glass particles. The volume resistivity decreased from 10^5 Ω cm at 5 vol% Ag@glass to (5.1 ± 0.3) 10^{-3} Ω cm at 15 vol% Ag@glass. Further increase in Ag@glass content decreased volume resistivity only marginally. The ECA containing 10 vol % Ag@glass and the halogen-based additive exhibited a yield stress of (51 ± 7) Pa, which increased to (236 ± 173) Pa at 15 vol% Ag@glass. At higher filler contents, the paste became tough and crumbly, rendering it unsuitable for application. The ECA with 15 vol% Ag@glass and halogen-based additive met the requirements for solar cell shingling in terms of volume resistivity and lap-shear strength ((20 ± 2) MPa), while utilizing only 2 vol% (14.4 wt%) silver. However, the yield stress of this formulation was rather high for printing or dispensing processes.

To overcome this issue, a possible approach to reduce yield stress of the ECA is dilution with a low-boiling solvent. However, solvent evaporation within a shingled joint is unfavourable. Instead, Ag@glass particles were mixed with Ag flakes to reduce the overall particle volume fraction while maintaining low volume resistivity. All formulations in the following experiments contained the halogen-based additive.

In a preliminary study, the total filler volume fraction was fixed at 5.0 and 6.7 vol%, respectively while the mixing ratio of Ag@glass to Ag flakes was varied. To meet the requirements of volume resistivity for a shingled solar cell interconnection of 10^{-2} Ω cm [26], a minimum of 3.5 vol% (app. 25 wt%) silver was required for such a low-filled ECA. The corresponding results are shown in Fig. S2.

Fig. 3b shows the volume resistivity of ECAs containing Ag@glass and Ag flakes with total particle volume fractions between 5 and 10 vol %. The Ag@glass-to-Ag flakes ratio was adjusted to maintain a constant total silver content of 3.5 vol%. The volume resistivity decreased from (9.6 ± 0.7) 10^{-3} Ω cm at 5 vol% total filler to (5.3 ± 0.5) 10^{-3} Ω cm at 10 vol%. Except for an outlier at 6 vol% with (1.1 ± 0.1) 10^{-2} Ω cm, the volume resistivity of all ECAs was below 10^{-2} Ω cm. The volume resistivity slightly decreases with increasing total particle volume fraction. Accordingly, the total silver fraction could be further reduced at a filler content above 8 vol% due to the higher amount of glass-core particles, that bring the silver shells into closer proximity. Additionally, the ECA with 8 vol% total filler exhibited a sufficiently low contact resistivity of (0.04 ± 0.01) mΩ cm^2.

The yield stress of these ECAs is shown in Fig. 4a. The yield stress increased exponentially from (22 ± 1) Pa at 5 vol% total filler to (148 ± 4) Pa at 10 vol%. All ECAs exhibited a superior lap-shear strength ranging from (20 ± 2) MPa at 5 vol% filler to (28 ± 3) MPa at 9 vol% filler (Fig. 4b). In all cases, cohesive failure was observed. Despite the increased particle content, which means higher number of potential defects in the polymer matrix, the lap-shear strength remained high. This is attributed to the better adhesion between Ag@glass particles and the epoxy than to Ag flakes. This conclusion is confirmed by lap shear strength measurements of samples containing 15 vol% of only Ag@glass or Ag flakes. The Ag@glass sample had a lap shear strength of (20 ± 2) MPa, which is twice as high as that of the ECA containing only Ag flakes ((10.1 ± 0.9) MPa).

Both volume resistivity and lap-shear strength showed only minor dependence on the glass fraction and remained within the required specifications. Therefore, the total filler fraction, determined by the

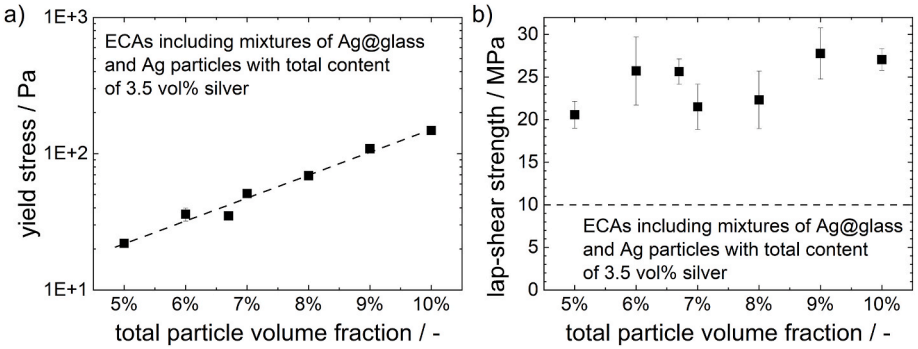

Fig. 4. a) yield stress and b) lap-shear strength of ECAs with varying total filler content between 5 and 10 vol% comprising Ag@glass and Ag particles at different mixing ratios to contain 3.5 vol% silver, higher total particle volume fraction corresponds to a higher fraction of Ag@glass particles in the mixture. The standard deviation of the yield stress measurements was too small to be visible in the diagram. Typically, the relative uncertainty of yield stress determination is in the order of 10%. Dashed line in diagram a) is to guide the eye, dashed horizontal line in diagram b) corresponds to the minimum required lap-shear strength for solar cell shingling.

additional glass content, can be taken to individually tune the rheological parameters. A yield stress between 10 and 100 Pa is recommended for dispensing and screen-printing application. ECAs containing 3.5 vol% silver and a total filler content of 5 to 8 vol% composed of Ag@glass and Ag flakes meet all requirements regarding rheological, electrical and mechanical properties in the uncured and cured state for shingled solar cell interconnection.

3.3. ECAs based on silver-coated copper particles

Further silver reduction was pursued by introducing silver-coated copper particles (Ag@Cu). These allow both shell and core to contribute to electron transport. However, the presence of copper presents challenges, including oxidation sensitivity and interactions with halogen additives, which may result in insulating compounds.

Suspending Ag@Cu particles in the epoxy resin used in this study resulted in ECAs without a yield stress and poor sedimentation stability. Consequently, samples for volume resistivity measurements were applied and cured immediately after mixing. The volume resistivity values shown in Fig. 5 thus represent the minimum volume resistivities achievable under proper stabilization. Sedimentation which occurred within minutes after mixing led to insulating samples. As reference, volume resistivities of ECAs containing Ag flakes are also shown in Fig. 5. ECAs containing Ag@Cu (15 wt% silver) were already conductive at a filler volume fraction of 5 vol% when cured directly after mixing. The volume resistivity at this filler content was (3.3 ± 0.2) 10^{-2} Ω cm and decreased to (1.11 ± 0.05) 10^{-3} Ω cm with increasing content of Ag@Cu up to 20 vol%. These results show, that ECAs based on silver-coated copper particles can meet the electrical requirements for shingled solar cell interconnection, provided that adequate stabilization against sedimentation is achieved. Obviously, the percolation threshold for the Ag@Cu particles is lower than that for the Ag flakes, this may be attributed to the smaller diameter of the Ag@Cu flakes or different surface chemistry.

Due to the chemical reactivity of copper, several non-reactive thickeners—namely fumed silica, carbon black, and Thixatrol AS 8053—were evaluated to improve particle stabilization. However, the increase in low-shear viscosity induced by these thickeners was not sufficient for particle stabilization. Additionally, the composites became insulating or did not fully cure. Detailed results are provided in the Supplementary Information (Figs. S3–S5). Despite copper's reactivity, the suitability of the halogen-based additive was investigated for ECAs containing silver-coated copper particles as well. Halogens can replace the fatty acids on the surface of the particles, leading to enhanced particle-particle interactions, morphological changes and increased electrical conductivity [36]. Careful adjustment of the halogen content resulted in the formation of a yield stress in the ECA based on Ag@Cu particles, effectively supressing particle sedimentation.

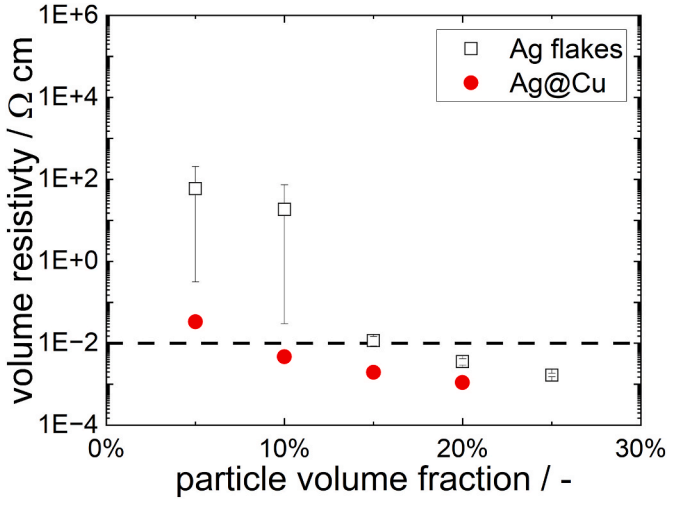

Fig. 5. Volume resisitivity of ECAs with Ag@Cu (filled red circels) and Ag flakes (un-filled black) with varying particle volume fraction from 5 to 25 vol%, samples were cured directly after mixing to prevent sedimentation, dashed line indicates the maximum volume resisitivty required for solar cell shingling. (For interpretation of the references to colour in this figure legend, the reader is referred to the Web version of this article.)

Fig. 6 summarizes the properties of this optimized ECA in comparison with commercially available ECAs and the requirements for shingled interconnection. The ECA contained 10 vol% of Ag@Cu particles, corresponding to a silver content of only 1.3 vol%. This is app. one quarter of the silver content of the commercial ECA with the lowest reported silver content (5 vol%) and more than an order of magnitude lower than that of standard highly-filled ECAs, which contain 20 to 30 vol% silver. In terms of weight, the ECA contained 7 wt% silver and 40 wt% copper. This formulation exhibited a volume resistivity of (4.3 ± 0.8) 10^{-3} Ω cm and a contact resistivity of (0.03 ± 0.01) mΩ cm^2, which satisfies the requirements for solar cell shingling. The yield stress of the ECA was (40 ± 11) Pa. The particles were thus stabilized against sedimentation and the ECA is suitable for screen-printing and dispensing. However, the curing kinetics of the ECA were altered, which led to a softer bond and a comparatively low Young's Modulus of (34 ± 13) MPa. DSC analysis revealed a shift of the main curing peak to higher temperature (126 °C instead of 106 °C) and the appearance of an additional shoulder above 150 °C (Fig. S3). Nevertheless, flexible bonds are preferred in shingled interconnection and the lap-shear strength of (28 ± 6) MPa was well beyond the required 10 MPa. The uncured ECA remained stable over more than six months when refrigerated at −20 °C and showed no degradation in volume resistivity after curing when stored under standard laboratory conditions for the same duration.

3.4. Application in shingled solar modules

To investigate the suitability of the developed ECAs for application in PV, especially solar cell shingling, mini modules with linear strings of six shingled cells were produced. The ECAs and their silver content as well as dispensed masses and volumes utilized for the three groups of modules are shown in Table 3. Twelve modules per formulations were produced for aging tests, plus two additional modules with the reference ECA serving as unaged reference modules. To obtain similar dispensing volumes with all three ECAs, dispensing parameters (pressure and preheat temperature) were adjusted to achieve dispensed volumes equivalent to the reference system.

SEM images of joint cross-sections are shown in Fig. 7. It is evident from the images that the particles were arranged in stacks forming conductive pathways. In the case of the Ag@glass ECAs, these stacks comprised Ag@glass and Ag flakes. Joint thickness was between 26 and 38 µm, wider than the average particle diameter. This indicates that current is conducted from particle to particle in all ECA formulations, which is typical for ECAs with a filler content beyond the percolation threshold.

The initial module performance is visualized in Fig. 8. Modules interconnected with Ag and Ag@glass ECAs demonstrated similar efficiencies of app. 19.64%. In contrast, modules with Ag@Cu ECA exhibited a marginally higher efficiency (Fig. 8a). Similarly, the module fill factors followed the same trend (Fig. 8b). Statistically, the observed differences between all experimental groups fall within one standard deviation of the mean values for both efficiency and fill factor, indicating no statistically significant variance in the initial module performance across the three ECA formulations.

To compensate calendar aging and the measurement error from the uncalibrated *IV* measurement, the failure criterion for ageing tests was set to a loss of $5\%_{rel.}$ compared to the unaged reference modules. Fig. 9 shows the aging test results along with the criterion derivation (solid red line) and failure threshold (dotted red line). After aTC 200 (Fig. 9a), Ag

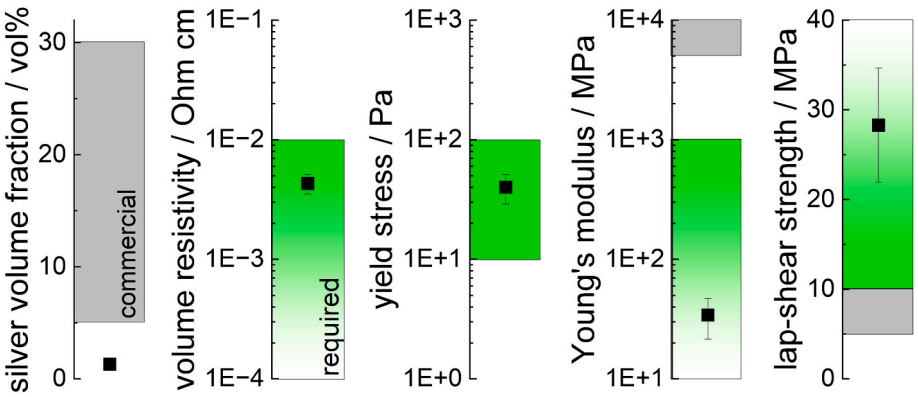

Fig. 6. Silver content as well as electrical and mechanical properties of the ECA with 10 vol% Ag@Cu and halogen additive indicated as black squares compared to commercial products (grey) and requirements for shingled solar cell interconnection (green). (For interpretation of the references to colour in this figure legend, the reader is referred to the Web version of this article.)

Table 3
Applied ECAs in the different module groups with their silver content and masses applied per shingle and calculated dispensed volume per shingle.

ECA formulation	Silver volume fraction/-	Silver weight fraction/-	Dispensed mass per shingle/mg	Uncured density/g/mL	Dispensed volume per shingle/μL
Ag (PROTAVIC® ACE 10720), reference	6.5-10%	40-50%	4.2 ± 0.2	1.78	2.4 ± 0.2
Ag@glass	3.5%	25%	3.6 ± 0.2	1.52	2.4 ± 0.2
Ag@Cu	1.7%	7%	4.1 ± 0.3	1.94	2.1 ± 0.2

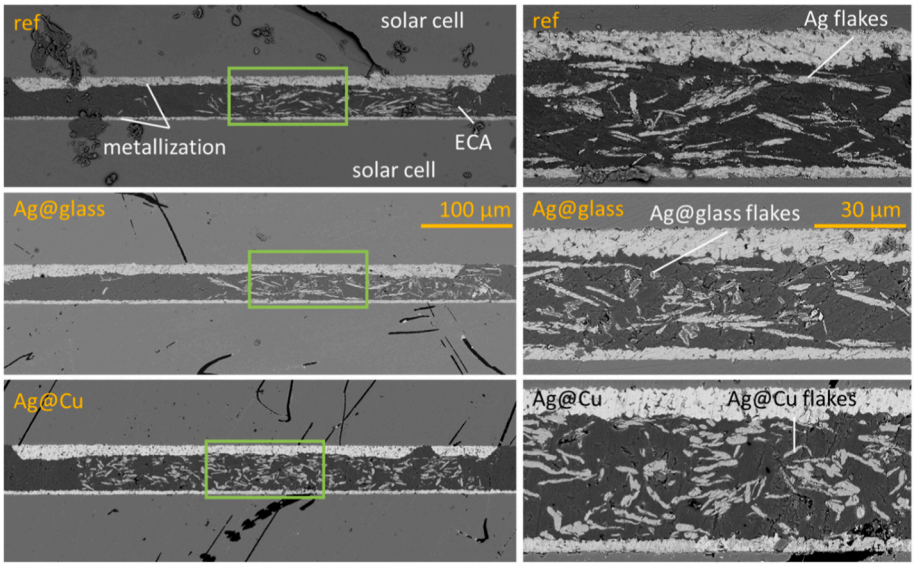

Fig. 7. SEM images of shingled solar cell joint cross-sections made from ECAs with Ag flakes, Ag@glass and Ag@Cu flakes, images on the left show the whole metallization, images on the right are magnifications of the left images at the position of the green square. (For interpretation of the references to colour in this figure legend, the reader is referred to the Web version of this article.)

and Ag@glass fillers demonstrated similar relative efficiency changes. In contrast, the Ag@Cu system exhibited significant performance degradation. One module showed no measurable power output after the test and thus is not shown in Fig. 9a and was excluded from further analysis. Three modules failed the test due to significant fill factor losses and thus efficiency losses. The fill factor degradation patterns (Fig. 9a) mirror those observed for module efficiency. This correlation between efficiency and fill factor degradation strongly indicates that the performance losses are primarily attributed to interconnection degradation. The Young's Modulus of the ECA filled with Ag@Cu ((34 ± 13) MPa) was significantly lower than that of the commercial silver-filled ECA (1400 MPa). This could have led to higher strains under thermo-mechanical stress, which might have interrupted the conductive pathways within the Ag@Cu filler system, leading to progressive deterioration of the electrical connectivity. Additionally, the different curing kinetics of the Ag@Cu ECA may have contributed to the observed stability issues, as insufficient cross-linking density could result in weakened polymer matrix integrity under thermal cycling conditions. Results from DH 500 testing are shown in Fig. 9b. All groups showed less than 5% efficiency loss. The stable fill factors after damp heat aging indicate that under these test conditions, oxidative degradation of the filler particles does not represent a limiting factor for any of the studied

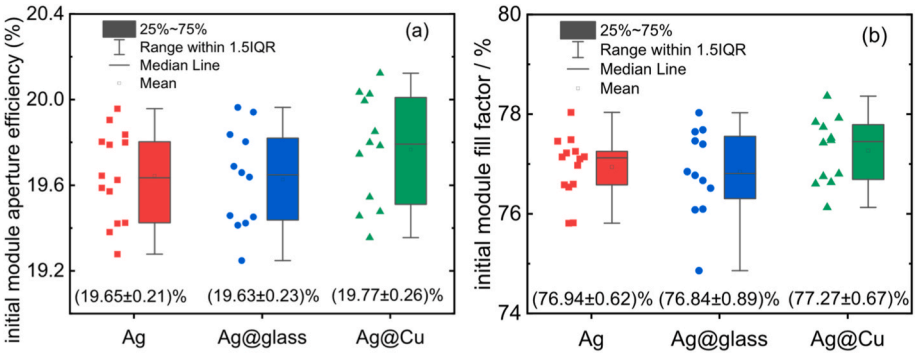

Fig. 8. Initial characterization of the produced six-shingle mini modules. (a): aperture efficiency, (b): fill factor. The individual data points are plotted next to bar plots, calculated from the same data. The median value and standard deviation of each group are written below the data.

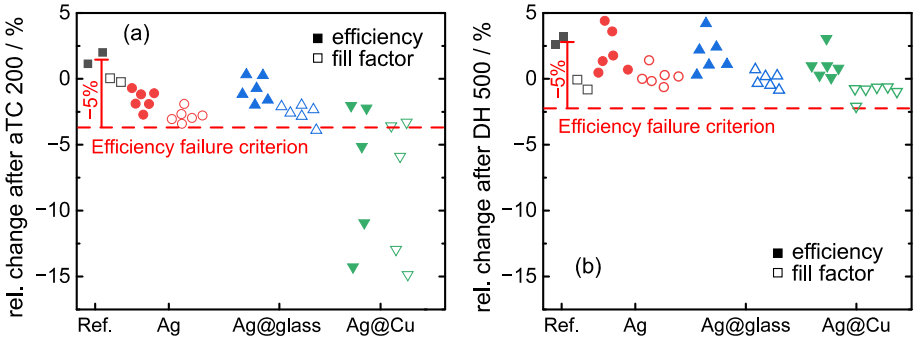

Fig. 9. Relative efficiency changes of six-cell mini modules after (a) aTC and (b) DH aging with failure criterion derivation (solid red line) and threshold (dotted red line). (For interpretation of the references to colour in this figure legend, the reader is referred to the Web version of this article.)

ECA systems.

4. Conclusion and outlook

Sustainable energy production requires sustainable material supply. Therefore, the PV industry aims to replace silver in metallization and interconnection of solar cells. However, up to date a full replacement of silver is not possible. Instead, core particles coated with a thin silver layer are utilized. These core particles can be either conductive or non-conductive. In this study, one of each type was evaluated.

Inert glass particles increase particle volume and bring the silver layer in closer contact. However, the particle volume required for conductivity led to a high yield stress, unsuitable for application. This was overcome by replacing only a part of the Ag flakes by Ag@glass. For a volume resistivity of 10^{-2} Ω cm, at least 3.5 vol% silver was necessary in ECAs with a total particle volume fraction below 8%. This led to an ECA containing only 25 wt% silver with lap-shear strength beyond 20 MPa and yield stress between the required 10 and 100 Pa, tuneable by the fraction of Ag@glass particles used.

Further reduction in silver content was achieved by utilizing silver-coated copper particles, as example for fillers with conductive cores. However, the formulation with copper is more challenging. The effect of thickeners was retarded in such systems or their application led to high resistivities or incomplete curing. By carefully adjusting the content of a halogen-based additive, an ECA was obtained containing 10 vol% of Ag@Cu, fulfilling all requirements for solar cell shingling at only 1.7 vol % (7 wt%) silver content.

In module evaluation, the formulated ECA systems utilizing Ag@glass or Ag@Cu particles showed similar initial performance as the Ag filled reference system. After aTC 200, while the Ag@glass system passed the test with similar power losses as the Ag system, the Ag@Cu system showed severe degradation. This could be due to insufficient mechanical stability of the conductive pathways under thermomechanical stress, leading to increased series resistance. DH 500 revealed that oxidative degradation is not a limiting factor for all three studied systems (all <5% loss), suggesting that the Ag@Cu degradation mechanism is primarily mechanical, not chemical.

Silver-coated glass particles are promising to replace pure silver flakes. With copper containing particles, interaction with the polymer becomes relevant. Other polymer-particle combinations providing better compatibility should be investigated in future studies to formulate a more reliable ECA with silver-coated copper particles. Furthermore, including nano-sized particles in addition to the micron-sized flakes could be addressed in future studies. On module level, it would be interesting to evaluate the ECAs on cells with low-temperature metallization (e.g. SHJ or silicon-perovskite tandem cells) and other encapsulants (e.g. TPO or POE) to study possible interactions between ECA, cell and encapsulant. Extending the aging experiment with the full test series specified in IEC 61215-1 would allow full qualification of the ECA for application in solar modules.

CRediT authorship contribution statement

Marianne Kronsbein: Writing – review & editing, Writing – original draft, Visualization, Investigation. **Leonhard Böck:** Writing – review & editing, Writing – original draft, Investigation. **Torsten Rößler:** Writing – review & editing, Supervision. **Norbert Willenbacher:** Writing – review & editing, Supervision, Funding acquisition.

Funding sources

This work was funded by the German Federal Ministry for Economic Affairs and Energy (BMWE) as part of the project “Mod30+” with the grant number 03EE1160.

Declaration of competing interest

The authors declare that they have no known competing financial interests or personal relationships that could have appeared to influence the work reported in this paper.

Acknowledgements

The authors like to thank Simon Malandain and Vincent Charlot and Frederic Durand of PROTAVIC INTERNATIONAL Laboratory for their professional support and material supply and Sofia Franceschini Mayr for conductance of experiments.

Appendix A. Supplementary data

Supplementary data to this article can be found online at https://doi.org/10.1016/j.solmat.2026.114228.

Data availability

The data that has been used is confidential.

References

[1] VDMA, International Technology Roadmap for Photovoltaic (ITRPV) 2024 Results, 2025. Frankfurt am Main.
[2] The silver institute, The Silver Survey 2025, The silver institute, Washington, 2025.
[3] S. Schwertheim, M. Scherff, T. Mueller, W.R. Fahrner, H.C. Neitzert, Lead-free electrical conductive adhesives for solar cell interconnectors, in: 2008 33rd IEEE Photovolatic Specialists Conference, vol. 3, IEEE, 2008, pp. 1–6, https://doi.org/10.1109/PVSC.2008.4922588. PVSC 2008. Proceedings.
[4] K.M. Broek, I.J. Bennett, M.J.H. Kloos, W. Eerenstein, Cross testing electrically conductive adhesives and conductive back-sheets for the ECN back-contact cell and module technology, Energy Proc. 67 (2015) 175–184, https://doi.org/10.1016/j.egypro.2015.03.301.
[5] L. Theunissen, B. Willems, J. Burke, D. Tonini, M. Galiazzo, A. Henckens, Electrically conductive adhesives as cell interconnection material in shingled module technology, in: 2018 AIP Conference Proceedings 1999, 2018 080003, https://doi.org/10.1063/1.5049305.
[6] D. Klosterman, L. Li, J.E. Morris, Materials characterization, conduction development, and curing effects on reliability of isotropically conductive adhesives, IEEE Trans. Compon. Packag. Manuf. Technol. 21 (1998). https://ieeexplore.ieee.org/stamp/stamp.jsp?tp=&arnumber=679028.
[7] U.S. Geological Survey, U.S. Geological Survey, Mineral Commodity Summaries, January 2025, U.S. Geological Survey, 2025.
[8] S. Chu, Materials as an Enabling Technology in Getting to net-zero GHG Emissions, 2024.
[9] Nagase CA, Nagase Chemtex America, 2025. https://nagasechemtex.com/wp-content/uploads/2024/07/Solar-Stringing-and-Shingling-Solar-Back-Contact.pdf.
[10] atom adhesives, atom adhesives AA-DUCT GS1. https://atomadhesives.com/aa-duct-gs1-silver-glass-sphere-coated-electrically-conductive-epoxy-adhesive/, 2025.
[11] United Adhesives, Inc., United adhesives eposolder. https://unitedadhesives.com/epoxy_eca.html, 2025.
[12] Parker Hannifin Corp, Parker electrically conductive sealants. https://ph.parker.com/us/en/series/electrically-conductive-sealants-and-rtv-silicone, 2025.
[13] Master Bond Inc., Masterbond EP79FL, 2025.
[14] B.V. Holland Shielding Systems, Holland shielding shieldoseal. https://hollandshielding.com/en/shieldoseal-130-g-plastic-cartridge, 2025.
[15] Soliani Emc s.r.l., Soliani CSA. https://www.solianiemc.com/wp-content/uploads/2024/03/SOL-08-Conductive-silicone-adhesives-r9.pdf, 2025.
[16] W. Chen, D. Deng, F. Xiao, Electrically conductive adhesives filled with surface modified copper particles, in: 2013 14th International Conference on Electronic Packaging Technology, IEEE, Dalian, China, 2013, pp. 288–291, https://doi.org/10.1109/ICEPT.2013.6756473.
[17] H.-M. Ren, K. Zhang, Y.M. Matthew, X.-Z. Fu, R. Sun, C.-P. Wong, Preparation and performance of Ag-coated Cu flakes filled epoxy as electrically conductive adhesives, J Sol State Light 1 (2014) 10, https://doi.org/10.1186/s40539-014-0010-9.
[18] C. Li, X. Gong, L. Tang, K. Zhang, J. Luo, L. Ling, J. Pu, T. Li, M. Li, Y. Yao, Electrical property enhancement of electrically conductive adhesives through ag-coated-cu surface treatment by terephthalaldehyde and iodine, J. Mater. Chem. C 3 (2015) 6178–6184, https://doi.org/10.1039/C5TC00593K.
[19] X.M. Zhang, X.-L. Yang, B. Wang, Electrical properties of electrically conductive adhesives from epoxy and silver-coated copper powders after sintering and thermal aging, Int. J. Adhesion Adhes. 105 (2021) 102785, https://doi.org/10.1016/j.ijadhadh.2020.102785.
[20] E.B. Choi, J.-H. Lee, Enhancement in electrical conductivity of pastes containing submicron Ag-coated Cu filler with palmitic acid surface modification, Appl. Surf. Sci. 415 (2017) 67–74, https://doi.org/10.1016/j.apsusc.2017.01.006.
[21] Y. Lin, S. Chiu, Electrical properties of conductive adhesives as affected by particle compositions, particle shapes, and oxidizing temperatures of copper powders in a polymer matrix, J of Applied Polymer Sci 93 (2004) 2045–2053, https://doi.org/10.1002/app.20670.
[22] W. Zhang, J. Liu, L. Zhang, J. Wang, Z. Zhang, J. Wang, H. Liu, H. Chen, M. Li, The synergistic effect of micron spherical and flaky silver-coated copper for conductive adhesives to achieve high electrical conductivity with low percolation threshold, Int. J. Adhesion Adhes. 114 (2022) 102988, https://doi.org/10.1016/j.ijadhadh.2021.102988.
[23] Z.S. Hamrah, M. Pourabdoli, V.A. Lashgari, M.H.D. Mohammadi, Effect of time, temperature and composition on the performance of conductive adhesives made of silver-coated copper powder, Int. J. Adhesion Adhes. 114 (2022) 103114, https://doi.org/10.1016/j.ijadhadh.2022.103114.
[24] Z.S. Hamrah, V.A. Lashgari, M.H.D. Mohammadi, D. Uner, M. Pourabdoli, Microstructure, resistivity, and shear strength of electrically conductive adhesives made of silver-coated copper powder, Microelectron. Reliab. 127 (2021) 114400, https://doi.org/10.1016/j.microrel.2021.114400.
[25] N. Cheng, Z. Sun, X. Yu, Q. Yu, J. Zhao, Effect of flake silver-plated copper particles on the property enhancement of electrically conductive adhesives, Phys. Chem. Chem. Phys. 25 (2023) 10022–10032, https://doi.org/10.1039/D3CP00209H.
[26] M. Kronsbein, L. Böck, K. Dyhr, T. Rößler, N. Willenbacher, Less is more: enabling low-filled electrically conductive adhesives for shingled solar cell interconnection using the capillary suspension concept, Sol. Energy Mater. Sol. Cell. 287 (2025) 113603, https://doi.org/10.1016/j.solmat.2025.113603.
[27] C. Yüce, N. Willenbacher, Challenges in rheological characterization of highly concentrated suspensions - a case study for screen-printing silver pastes, JoVE J. (2017) 55377, https://doi.org/10.3791/55377.
[28] M.I. Devoto, T. Timofte, A. Halm, D. Tune, Improved measurement of the contact resistivity of ECA-based joints. https://doi.org/10.4229/EUPVSEC20212021-4BO.5.6, 2021.
[29] ASTM International, Standard test method for apparent shear strength of single-lap-joint adhesively bonded metal specimens by tension loading (Metal-to- metal). https://doi.org/10.1520/D1002-10R19, 2010.
[30] DIN-Normenausschuss Kunststoffe (FNK), Plastics Standards Committee, DIN EN ISO 20753 Kunststoffe - Probekörper, 2024.
[31] C.H. Schiller, L.C. Rendler, D. Eberlein, G. Mülhöfer, A. Kraft, D.-H. Neuhaus, Accelerated TC test in comparison with standard TC Test for PV modules with ribbon, wire and shingle interconnection, 36th European Photovoltaic Solar Energy Conference and Exhibition 995–999 (2019), https://doi.org/10.4229/EUPVSEC20192019-4AV.1.8, 5 pages, 4421 kb.
[32] D. Lu, Q.K. Tong, C.P. Wong, A study of lubricants on silver flakes for microelectronics conductive adhesives, IEEE Trans. Compon. Packag. Technol. 22 (1999) 365–371, https://doi.org/10.1109/6144.796536.
[33] C.P. Wong, D. Lu, Q.K. Tong, Lubricants of silver fillers for conductive adhesive applications. https://doi.org/10.1109/adhes.1998.742025, 1998.
[34] C. Yang, Y.-T. Xie, M.M.-F. Yuen, B. Xu, B. Gao, X. Xiong, C.P. Wong, Silver surface iodination for enhancing the conductivity of conductive composites, Adv. Funct. Mater. 20 (2010) 2580–2587, https://doi.org/10.1002/adfm.201000673.
[35] H. Sun, X. Zhang, M.M.F. Yuen, Enhanced conductivity induced by attractive capillary force in ternary conductive adhesive, Compos. Sci. Technol. 137 (2016) 109–117, https://doi.org/10.1016/j.compscitech.2016.10.028.
[36] J. Marten, J.S. Urallar, T.M. Duong, P. Théato, N. Willenbacher, Iodine-Induced microphase separation controls the flow behavior and electrical conductivity of silver-filled polymer composites, ACS Appl. Mater. Interfaces (2025), https://doi.org/10.1021/acsami.5c09040.